9

Research Article

Pethampalayam Karuppanan Miniappan, Sivagnanam Marimuthu*, Selvan Dharani Kumar, Gopal Gokilakrishnan, Shubham Sharma*, Changhe Li, Shashi Prakash Dwivedi, and Mohamed Abbas*

Mechanical, fracture-deformation, and tribology behavior of fillers-reinforced sisal fiber composites for lightweight automotive applications

https://doi.org/10.1515/rams-2023-0342 received February 01, 2023; accepted July 06, 2023

Abstract: The main focus of this study is on the effects of fly ash, basalt powder, and tungsten carbide (WC) on the mechanical (tensile strength, flexural strength, impact strength, and Shore D hardness) and tribology behavior of sisal fiber-reinforced composites. Using epoxy resin, the fillers (5–10 wt% of each) were mixed with sisal fiber and resin (30 wt%). A tensile strength of 86.3–112.2 MPa was observed with the addition of fly ash, basalt powder,

* Corresponding author: Sivagnanam Marimuthu, Department of Mechanical Engineering, Karpagam Academy of Higher Education, Coimbatore, India, e-mail: drsmarimuthu@gmail.com

Pethampalayam Karuppanan Miniappan: Department of Mechanical Engineering, Karpagam Academy of Higher Education, Coimbatore, India **Selvan Dharani Kumar:** Centre for Machining and Material Testing, Department of Mechanical Engineering, KPR Institute of Engineering and Technology, Coimbatore, India

Gopal Gokilakrishnan: Department of Mechanical Engineering, Sri Eshwar College of Engineering, Coimbatore, India

Changhe Li: School of Mechanical and Automotive Engineering, Qingdao University of Technology, 266520, Qingdao, China, e-mail: sy_lichanghe@163.com

Shashi Prakash Dwivedi: Department of Mechanical Engineering, Lloyd Institute of Engineering & Technology, Knowledge Park II, Greater Noida, Uttar Pradesh 201306, India, e-mail: spdglb@gmail.com

and WC fillers. The tensile strength of S2 composite (basalt powder + epoxy resin) was 33.63% higher than that of composite without fillers. The flexural strength of S5 composite (basalt powder + WC) was found to be 166.4 MPa, which is nearly 19.95% higher than the composite without filler. The fly ash with WC (S4) and basalt powder (S5) composite showed similar impact strength (5.34 J·m⁻²), which was nearly 62% greater than the composites without filler. The superior hardness was noticed in S5 composite compared to all other filler-added composites. The least wear rate was noticed in S3 (WC) composites irrespective of all the loading conditions. The hybridization of fillers also enhanced the mechanical properties of sisal fiber-reinforced composites. However, single filler-reinforced composite (WC) improved the wear resistance compare to hybrid filler-reinforced composites. The inclusion of filler increases the load-carrying capability and adhesion, as determined by scanning electron microscope. The river-like pattern confirms that S2-composite failure was dominated by ductile. The least wear debris and grooved surfaces were results higher wear resistance in the hybrid filler-reinforced composites.

Keywords: sisal fiber, epoxy resin, fillers, mechanical properties, SEM

1 Introduction

Composites of synthetic fiber-reinforced polymer are used in aerospace and vehicle applications. Despite possessing strong mechanical properties and a higher resilience to environmental ageing, these fiber composites are both environmentally and humanly dangerous. Researchers are currently using natural fibers as reinforcement for polymer-based composites. Natural fibers are superior

^{*} Corresponding author: Shubham Sharma, Mechanical Engineering Department, University Centre for Research and Development, Chandigarh University, Mohali, Punjab, 140413, India; School of Mechanical and Automotive Engineering, Qingdao University of Technology, 266520, Qingdao, China; Department of Mechanical Engineering, Lebanese American University, Kraytem 1102-2801, Beirut, Lebanon, e-mail: shubhamsharmacsirclri@gmail.com, shubham543sharma@qmail.com

^{*} Corresponding author: Mohamed Abbas, Electrical Engineering Department, College of Engineering, King Khalid University, Abha 61421, Saudi Arabia, e-mail: mabas@kku.edu.sa

to synthetic fibers because they are durable, biodegradable, inexpensive, and lightweight [1]. These fibers are excellent while using as reinforcement materials in the production of polymer composites that are suited for a variety of lightweight applications, including aircraft seats and automobile components [2-8]. The disadvantages of natural fiber-reinforced composites are fiber delamination, low modulus, water absorption, and limited application to low load-bearing materials [9-11]. With various polymer resin matrices [12–16], natural fibers such as sisal, banana, cotton, ramie, jute, pineapple, kenaf, coir, and bagasse were utilized. Sisal fiber-reinforced polymer composites exhibit remarkable advantages in their mechanical properties compared to composites reinforced with other natural fibers [17]. These fibers include a greater proportion of cellulose components, which is the reason for their enhanced tensile properties, and they do not absorb moisture quickly. Sisal fibers have been widely used as reinforcement in cementitious composites [18,19] in recent years. The type of fibermatrix bond is principally responsible for determining the qualities of sisal fibers. There are a number of factors, including surface treatment, fiber length, strengthening, and filler addition [19]. Sisal can be cultivated easily, and its timing of plantation is less [17]. A study showed that sisal fiber is extracted globally at a rate of about 4.5 million tonnes annually [20]. It comes from the leaves of the sisal plant (Agave sisalana), which is presently grown in tropical African, West Indian, and Far Eastern countries [21]. Noorunnisa Khanam et al. [22] studied the influence of chemical treatment on the mechanical behavior of sisal fiber-reinforced composites. Sisal fiber boiled in 18% aqueous NaOH exhibited improved tensile and flexural strength. The capacity of the sisal fiber to attach was enhanced by the NaOH treatment. Sisal fiber-reinforced composites did not have the same tensile strength as synthetic fiber-reinforced composites [23,24]. The natural fiber-reinforced composite was augmented with fillers to increase its mechanical qualities [17]. According to Maurya et al. [25], the addition of fly ash to sisal fiber-reinforced composites enhanced their tensile and flexural strengths. Fly ash with 46% silica displayed superior tensile and flexural characteristics with epoxy-based composites up to a 3% additive level [19]. Devaraju and Sivasamy [26] studied the effect of nanoparticles (ZrO2 and ZnO) on mechanical properties of sisal fiber composites. They concluded that the mechanical properties of ZrO₂ sisal fiber composite were higher than those of ZnO sisal fiber composites. Ji et al. [27] studied the mechanical and water absorption properties of sisal fiber composite that contains fillers such as talcum powder, CaCO₃, and eggshell powder. The addition of fillers improved the mechanical and water resistance properties of the sisal fiber composites. Alemayehu

et al. [28] concluded that sisal fiber composite was good replacement material for vehicle body applications. Athith et al. [29] determined that natural fibers and tungsten carbide (WC) fillers enhanced the characteristics of hybrid composites (jute/sisal/E-glass). The bagasse ash-filled composite reinforced with sisal, flax, banana, and kenaf considerably enhanced the composite material's thermal and mechanical qualities [30]. The addition of up to 3 wt% bagasse ash to composites resulted in increased tensile, flexural, and impact strengths [30]. Haldar et al. [31] evaluated the mechanical characteristics of sisal fiber-reinforced composites with and without the addition of aluminum powder. The filler substance enhances fiber-matrix adhesion and decreases void volume. Oladele et al. [32] examined the mechanical and wear properties of CaCO₃-filled, sisalfiber composites. The tensile, flexural, and hardness properties of the composite were improved by the inclusion of CaCO₃ filler. However, the impact properties of composites were noticed. da Silva et al. [33] enhanced the mechanical characteristics of the sisal fiber-reinforced composites by adding silica micro-particles. Mohan and Kanny [34] observed that the addition of nanoclays to sisal fiber-reinforced composites led to a slight increase in tensile strength.

It appears that there are few studies in the literature about how fillers influence the mechanical, tribology, and physical characteristics of sisal fiber composites. But there have not been many studies done on basalt and WC filler used in sisal fiber-reinforced composites. The hybridization of filler materials such as fly ash, basalt powder, and WC with sisal fiber reinforcement has been found to be very low. In this work, organic fillers (fly ash, basalt powder) and inorganic filler (WC) were used to study their effect on the tensile, flexural, impact, hardness, and wear properties of sisal fiber-reinforced composites. In addition, the mechanical properties and tribology behavior of sisal fiber-reinforced composites are also studied, and the results are compared to those of composites without filler. The tensile fracture and wear pattern of hybrid fillerreinforced composites are also examined in detail.

2 Materials and method

Sisal fiber used as reinforcement was purchased from Go Green Products, Chennai, India. Before processing, these fibers were soaked in a 2% NaOH solution for 24 h at room temperature to improve the interfacial bonding between the fiber and matrix, which resulted in improved mechanical properties [35,36]. After that, these fibers were rinsed with distilled water and then dried in a hot oven at a temperature of 60°C. The dried fibers were

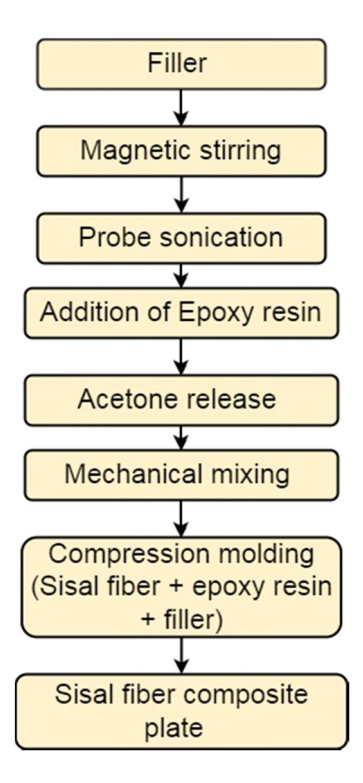


Figure 1: Manufacturing steps of filler reinforced composites.

chopped into 20-25 mm lengths and used in composite fabrication. The hardener (HY951) and epoxy resin (LY556) were purchased from Covai Seenu & Company in Coimbatore, India. The coal-fired fly ash was collected from power plants. The fly ash was separately ground using a ball milling machine. WC (size, 2 µm; purity, 99%) was purchased from Ultrananotech Private Limited, India. The steps followed for filler dispersion and composite manufacturing are shown in Figure 1. The filler was mixed with acetone by using a magnetic stirrer for 20 min and then a probe sonicator for 20 min. Following the addition of sufficient epoxy resin, this mixing process was carried out excessively. Finally, the hardener was mixed with epoxy + filler. Nonsilicone white wax was applied inside the mold to avoid adhesion of the mixture to the mold. After applying the wax, the fiber was arranged in the mold of the compression

molding machine. The epoxy + filler + hardener mixture was poured inside the mold. The operating parameters used for manufacturing all composites in this study were pressure (15 MPa) and temperature (120°C).

The same fabrication procedure was adopted for all six samples, and details of all the samples are listed in Table 1. The presence of filler in the S4, S5, and S6 composites was confirmed by the energy dispersive X-ray spectroscopy (EDS) results as shown Figure 2(a-c).

After the composites were cured, they were sliced into plates for testing. All mechanical testing samples were cut as per the ASTM standard, and cutting was done using a water jet cutting machine. Using Aimil universal testing equipment, the tensile and flexural strengths of each sample were tested in accordance with ASTM 3039 [1] and ASTM 790 [1], respectively. The impact resistance of the samples was determined using a digital Izod impact tester in accordance with ASTM D-256 [17]. Using a Shore D hardness tester, Shore D hardness testing was conducted in accordance with ASTM D2240 [1]. The dry wear test was conducted using pin-on-disc equipment (DUCOM machine) in accordance with ASTM G99 specifications. The samples measured 15 mm × 5 mm × 5 mm and were perpendicularly drilled into an EN-32 steel disc with a 50-mm track diameter. Using scanning electron microscopy (SEM), the tensile fracture and worn surfaces were studied.

3 Results

3.1 Tensile results

Figure 3(a and b) depicts the stress versus strain graph and specimens after the tensile test. Figure 4 displays the results of the evaluation of the tensile several sisal fiber polymer composites. Without the inclusion of filler components, the tensile strength of composites reinforced with sisal fiber epoxy was 83.96 MPa [37]. However, the inclusion of fly ash, basalt powder, and tungsten carbide fillers

Table 1: Sample designation and compositional details

S. No	Sample designation	Polymer composites
1	S1	Epoxy (70 wt%) + Sisal fiber (20 wt%) + Fly ash (10 wt%)
2	S2	Epoxy (70 wt%) + Sisal fiber (20 wt%) + Basalt powder (10 wt%)
3	S3	Epoxy (70 wt%) + Sisal fiber (20 wt%) + Tungsten carbide (WC) (10 wt%)
4	S4	Epoxy (70 wt%) + Sisal fiber (20 wt%) + Fly ash (5 wt%) + Tungsten carbide (5 wt%)
5	S5	Epoxy (70 wt%) + Sisal fiber (20 wt%) + Fly ash (5 wt%) + Basalt powder (5 wt%)
6	S6	Epoxy (70 wt%) + Sisal fiber (20 wt%) + Tungsten carbide (5 wt%) + Basalt powder (5 wt%)

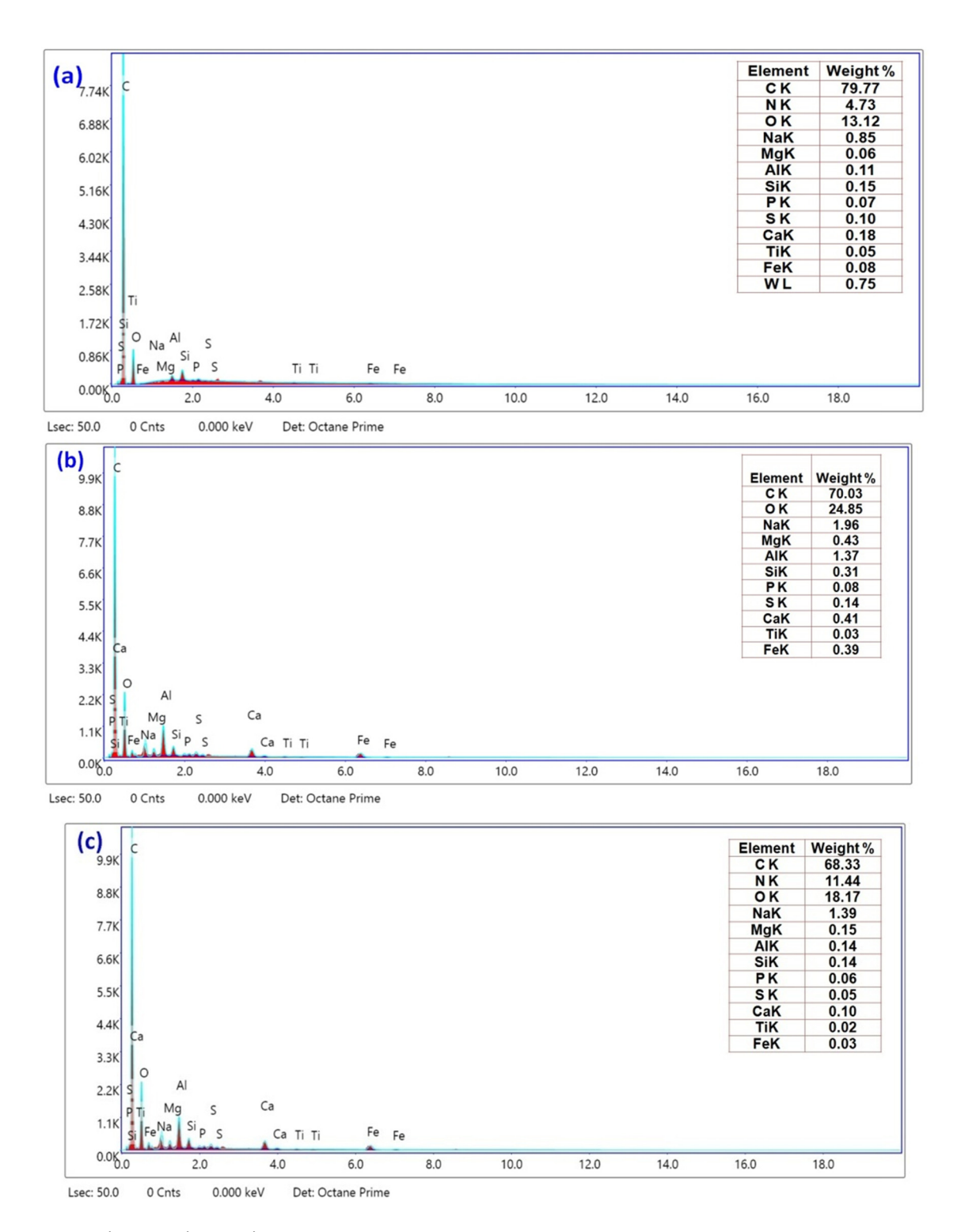


Figure 2: EDS results: (a) S4, (b) S5, and (c) S6.

in the sisal fiber epoxy-reinforced composites boosted their tensile strength in comparison to those without fillers. Maximum tensile strength of 112.2 MPa was recorded for S2 composites with 10 wt% basalt powder, an increase of almost 33.63% compared to sisal fiber polymer composites without

filler. S1 (10 wt% fly ash) and S3 (10 wt% WC) composites had the lowest tensile strength compared to the other composites. The reduced tensile strength of the S1 composites was caused by an increase in fly ash content of more than 5 wt%. Among all, the lowest tensile strength was noticed in the S3 (WC).

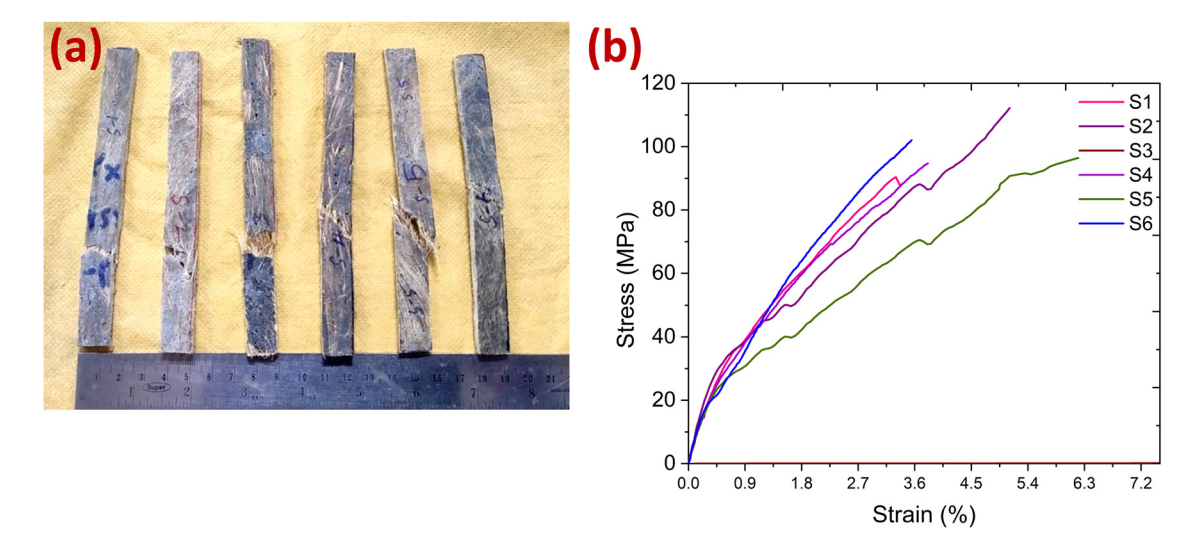


Figure 3: Tensile test: (a) specimens and (b) stress-strain curves.

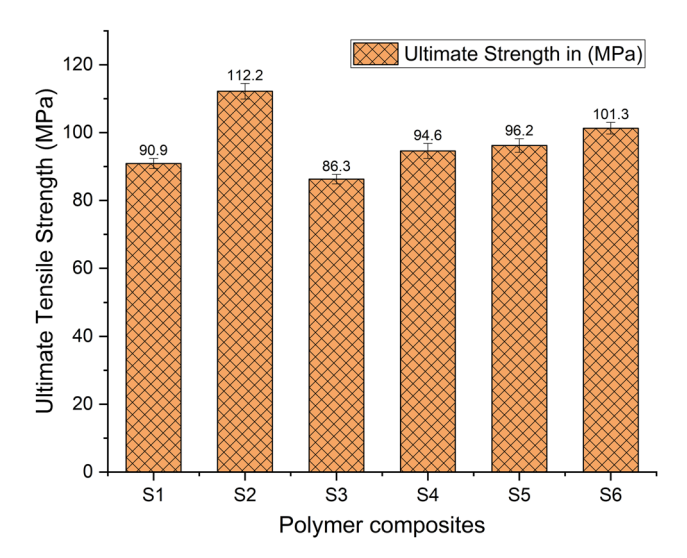


Figure 4: Tensile results.

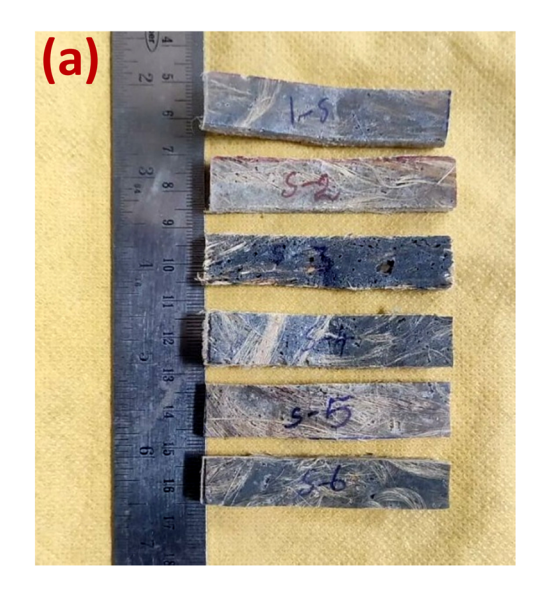
Due to insufficient wetting of WC during tensile loading, the interfacial adhesion between sisal fibers and matrix was weakened, resulting in decreased tensile strength. Similar cases were reported in sisal-reinforced epoxy composites [38]. The improper mixing of the fly ash and WC may be the reason for the lower strength as compared to the basalt powder. S2 (10 wt% basalt powder) had a tensile strength that was 23.43 and 30.01% higher than the S1 and S3 composites, respectively. The combined effect of two fillers in the reinforced composites (S4, S5, and S6) enhanced the tensile strength as compared with single filler-reinforced composites (S1 and S3). However, it was less than the S2 composites. Despite the presence of two fillers in the sisal fiber reinforced composites, basalt powder was the most dominant

filler material, followed by fly ash and WC. The basalt with WC (S6) composites showed the second-highest tensile strength. The addition of fly ash filler to basalt (S4) and WC (S5) composites did not significantly increase the tensile strength in comparison to other composites (WC + basalt powder). Finally, it was discovered that the fly ash filler does not maintain effective load transfer during composite tensile testing [38]. Basalt powder was the most effective filler compared to other fillers used in this study. Because of repulsion, the fly ash and WC fillers' likely agglomeration decreases as the cationic surfactant percentage increases. Inorganic also fills the matrix's meso and microvoids, strengthening the composites' excellent packing.

3.2 Flexural results

Figure 5(a and b) depict the stress *vs* strain graph and specimens after the tensile test. Figure 6 illustrates the flexural strength of several composites reinforced with sisal fiber. The flexural strength of sisal fiber-reinforced composites was 138.72 MPa without any filler [22].

The results demonstrate conclusively that fly ash, basalt powder, and WC increased the flexural strength of sisal fiber composites. The superior flexural strength of the S5 composite was found to be 166.4 MPa, which was nearly 19.95% greater than composites without the addition of filler material. The second-highest flexural strength was noticed in the S2 and S4 composites. The flexural strength of fly ash + WC reinforced composites and basal powder composites did not differ significantly. The least flexural



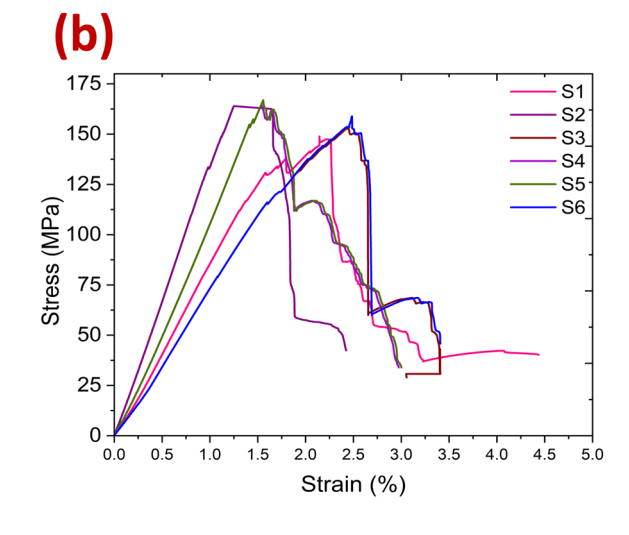


Figure 5: Flexural test: (a) specimens, (b) stress-strain curves.

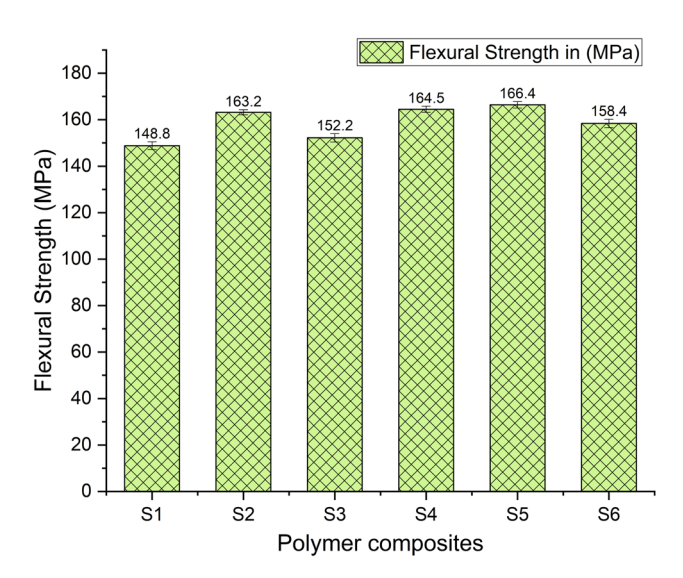


Figure 6: Flexural results.

strength was noticed in the fly ash (S1) and WC (S3) filler-reinforced composite (S1). The improved load transmission and elastic deformation of the sisal fiber-reinforced composite [17] were attributed to the increased interfacial stiffness and better adherence of fly ash powder at smaller particle sizes. Therefore, it was the primary reason for the reduced flexural strength of composites reinforced with fly ash. In addition, the addition of WC, fly ash, and basalt powder to the composites decreased their flexural strength. The accumulation of WC renders the composite more brittle and decreases the sisal fiber's rigidity. James *et al.* [39] discovered that eliminating contaminants and

brittle particles from sisal fiber hybrid composites increases their flexural strength.

The basalt powder filler boosted the composite's flexural strength in comparison to other fillers. In addition to other fillers, the filler boosted the flexural strength of the composite. Basalt powder bonds sisal fiber and epoxy resin efficiently at their interfaces. Vivek and Kanthavel [30] saw a similar effect, where the flexural strength of basalt powder-reinforced natural fiber composites which were depended entirely on how well the filler stuck to the fiber and matrix. The main factor in the composite's ability to maintain its stiffness attributes was the filler's strong interfacial bonding with sisal fiber and epoxy resin.

3.3 Impact results

Figure 7(a and b) depicts the impact test samples and results of sisal fiber-reinforced composites with various fillers. The results clearly demonstrate that the presence of fillers increased the impact strength of the composites in comparison to composites without filler. Without fillers, Gupta and Srivastava [37] observed that the impact strength of sisal epoxy-reinforced composites was 2 kJ·m⁻². S4 (fly ash + WC) and S5 (fly ash + basalt powder) composites demonstrated maximum impact strengths of 5.34 J·m⁻², which were nearly twice as high as the composites without filler. Single-filler composites (S1, S2, and S3) had lower impact strength than composites with two fillers (S4 and S5). S1 and S2 composites showed the least impact strength compared to other composites. S1 (fly ash), S2 (basalt powder), S3 (WC), S4 (fly



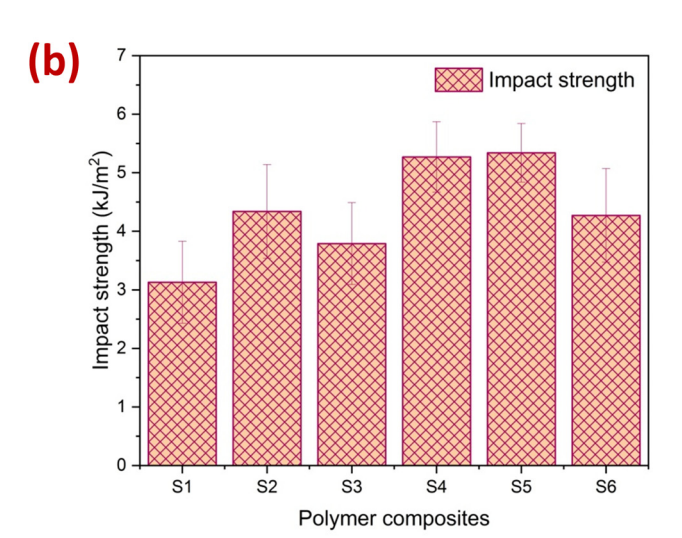


Figure 7: Impact test: (a) samples and (b) impact results.

ash + WC), S5 (fly ash + basalt powder), and S6 (WC + basalt powder) improved their impact strengths by 36.10, 65.19, 47.22, 62.04, 62.54, and 53.16%, respectively. Normally, voids form during the production of composites reinforced with natural fibers [38]. These voids may increase the stress and accelerate the formation and propagation of cracks. Fillers significantly inhibit crack formation and propagation in sisal fiber-reinforced composites by effectively filling these voids.

Fillers can function as a connecting link between the fiber and matrix, which increases interfacial adhesion and contributes to the enhancement of impact strength. The increase in impact resistance may be attributable to the fact that fillers absorb energy due to their higher surface-to-volume ratio [33]. The reduction in impact strength in S3 was due to insufficient wetting and agglomeration.

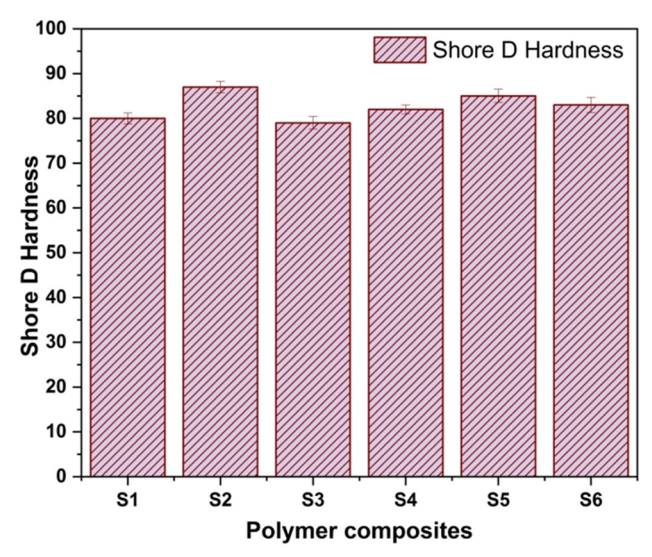


Figure 8: Shore D hardness test results.

3.4 Shore D hardness test results

Figure 8 illustrates the effect of fillers on the Shore D hardness of sisal fiber reinforced composites. The sisal fiber epoxy-reinforced composite had a Shore D hardness of 77.3 [39].

The addition of filler materials such as fly ash, basalt powder, and WC to the composite enhanced its hardness properties as compared with sisal fiber composites without filler. With the addition of fillers, the polymer and fiber chains are held in place, which makes the composite stiffer and harder. It was noticed that, over composites without filler, the average Shore D hardness was increased by 3.375% (S1), 11.149 % (S2), 2.15% (S3), 5.73% (S4), 9.05% (S5), and 6.86% (S6) for composites with filler added composites. Basalt filler reinforced composite showed a significant improvement as compared to fly ash and WC. The improper dispersion of WC fillers at minor loading resulted in increased inter-particle distance, which was the primary reason for inferior hardness in the S3. The decrease in hardness in the S4, S5, and S6 composites may be attributed to filler heterogeneities that result in a higher void content in the composites. Megahed et al. [40] showed comparable increases in hardness values for sisal fiber composites.

3.5 Wear test results

In this study, the dry wear test was carried out on a pin-ondisc apparatus. Figure 9(a and b) depicts the pin-on-disc apparatus and samples. The samples were subjected to the

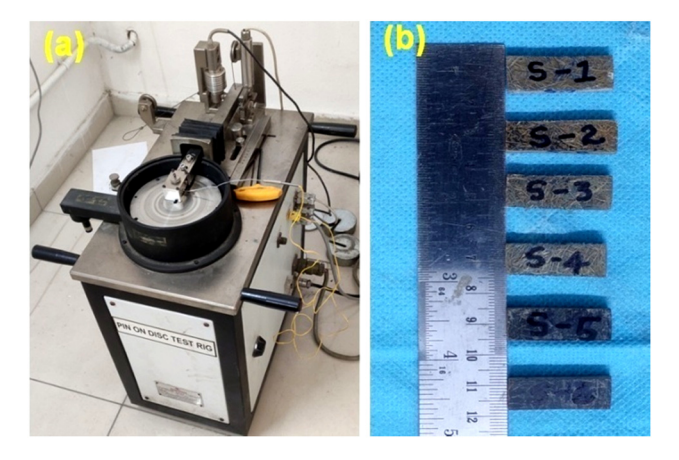


Figure 9: (a) Pin-on-disc and (b) samples.

respective normal load and sliding velocities of 10, 20, and 30 N and 150, 250, and 350 rpm for the wear test.

Important operational parameters for the wear of polymer composites included the applied load and sliding velocity. Therefore, it was varied by a constant sliding distance of 700 m. In each combination, approximately three specimens were evaluated, and the average value was recorded. Figure 10 demonstrates that the wear rate of all sisal fiber composites rises sharply with increasing normal load and sliding velocity. S1 composites have the highest wear rate, whereas S4 composites have the lowest wear rate for all combinations of normal loads and sliding velocity. The highest wear rate was found in the S1 composite (1,450 µm) at 30 N load and 350 rpm. However, the least wear rate was obtained in the S4 composite (84 µm) at 10 N load and 150 rpm. The wear rate of S4 remains between 84 and 273 µm at lower sliding velocity (150 rpm) while the wear rate remains between 360 and 920 µm at higher

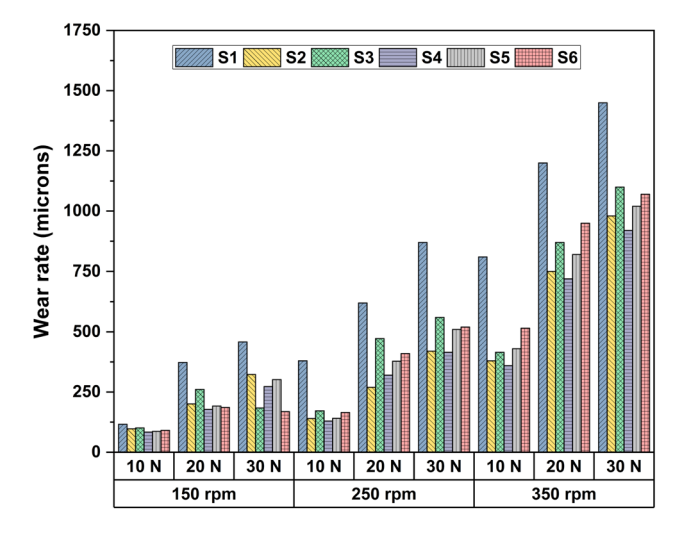


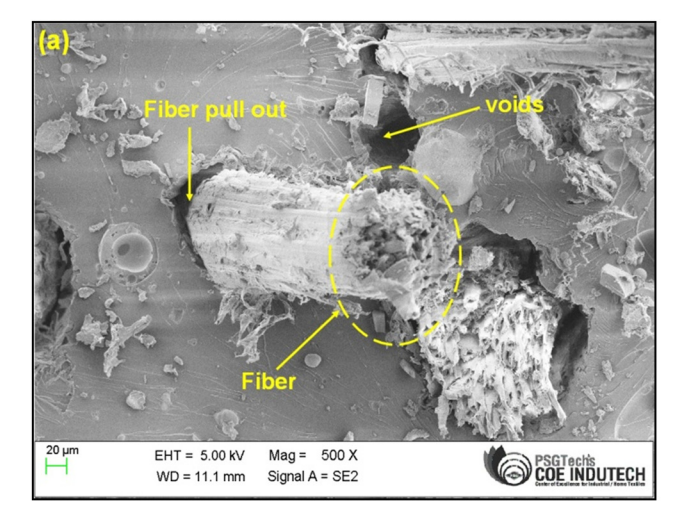
Figure 10: Wear rate of sisal fiber polymer composites.

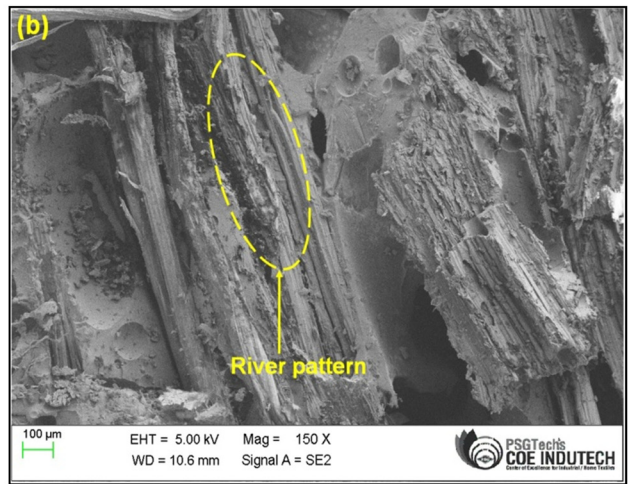
sliding velocity (350 rpm) respective of the normal load (10-30 N). The sisal fiber epoxy matrix interphase was strongly incorporated by the WC with fly ash fillers, providing transfer films on the material surface that reduced wear resistance under all loading circumstances. Similar kinds of results were observed by Govindan et al. [41]. Next to S4, the least wear rate was observed in the S5 composites at lower sliding velocity (150 rpm) irrespective of normal load. However, compared to S5, the wear rate of S2 was lower at higher sliding velocity and normal load. It was confirmed that the wear behavior of the S2 composite was gradually reduced at higher loading conditions. The decrease in wear resistance of the S5 composite at higher loading conditions was mainly due to an increase in contact area and less abrasion resistance of fly ash. The wear rate of S2, S5, and S6 composites is in the range of 1020-1100 µm. The basalt powder was added to the S2, S5, and S6 composites. However, the wear rate of the S2 composite was higher than S5 and S6. The hybridization of filler material was the reason for a slight increase in the wear resistance of S5 and S6. The highest wear rate was noticed in S1 composites irrespective of all the loading conditions. S1 composites decreased the resistance to abrasion due to the inclusion of fly ash filler. This can be a result of an increase in the resin's effective contact area and a suitable filler level in the frictional composition. The abrasion resistance of fly ash was lower than the WC and basalt powder. From the wear studies, it was determined that filler materials can lower the stress on sisal fibers and avoid thermal and mechanical breakdown of the matrix in the contact region. SEM was used to analyze the sample's worn surfaces in order to better comprehend the likely wear process and material loss.

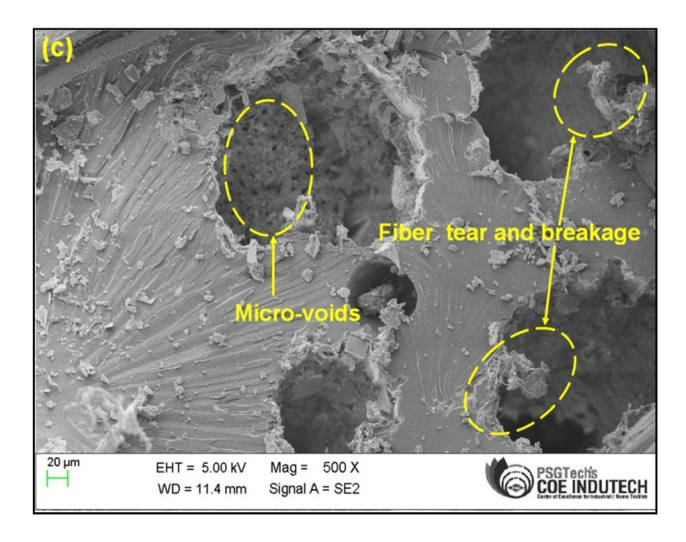
3.6 SEM tensile fracture results

Figure 11(a–c) depicts the SEM fracture surfaces of the tensile samples S1, S2, S3, and S4 of sisal fiber-reinforced composites (d).

A weak interfacial interaction between sisal fiber and epoxy matrix allowed the fiber to separate from the matrix. The creation of voids is one of the reasons why S1 samples have a lower tensile strength. The existence of voids confirms that the S1 sample failed to fracture in a responsible way. On the fracture surfaces of S2 samples, a river-like pattern is visible (Figure 11b). The occurrence of a river-like pattern confirms the failure was dominated by the ductile. A similar kind of failure was noticed in the graphene filler added to banyan aerial root fiber composites [1]. The cohesiveness of the matrix in the S2 sample is better, and this is confirmed by







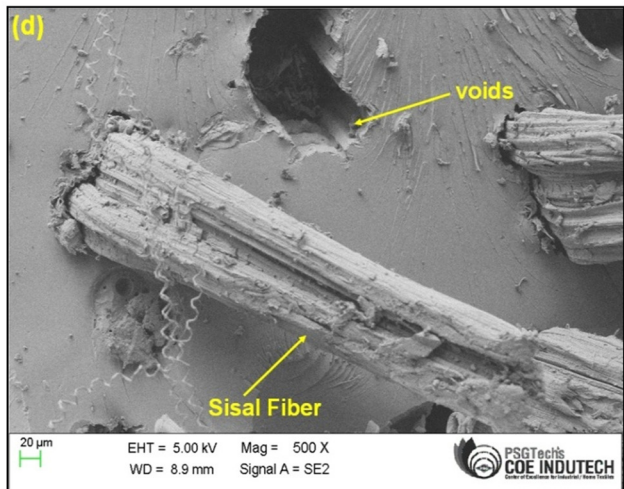


Figure 11: Tensile fracture SEM: (a) S1, (b) S2, (c) S3, and (d) S4.

the presence of a river pattern on the fracture surface. Clearly, a portion of the fibers have been split, enhancing their load-bearing qualities. Figure 11(c) shows the fiber tear and breakage along with voids. The fiber tear and voids were the main reason for the decrease in tensile strength. The fiber breakage on the fracture surface confirmed that the adhesion between fiber and matrix was superior in the S3 sample. No fiber breakage is noticed on the S4 fracture surface. However, the presence of voids in the fracture surface was the primary reason for the drop in tensile strength, even though there was no fiber breakage or cracks.

3.7 SEM results of worn surfaces

Figure 12(a–f) depicts the worn surfaces of all sisal fiber composites subjected to maximum conditions at a normal load of 30 N and sliding velocity of 350 rpm.

The wear debris, cracks, and large grooved surfaces are noticeable in the S1 composite (Figure 12(a)). It confirms that a larger surface is worn due to a higher wear rate. It reveals that a larger surface was worn because the wear rate was higher. The surfaces cracking with grooved surfaces are seen in the S2 composites (Figure 12(b)). Deeply grooved grooves on the worn surfaces lead to a higher composite wear rate. Renukappa et al. [42] observed a similar sliding wear mechanism in nanoclay filler-added epoxy composites. The absence of wear debris confirmed the wear rate of S2 was less compared to S1. The worn surface of S3 composite (Figure 12(c)) was completely different from those of S1 and S2. The wear debris was found in a large portion, along with surface deformation and micro-voids. From this, it was clearly noticed that the binding of the WC filler in the epoxy resin was less than that of the other two fillers. The occurrence of surface deformation is the major cause of predominant wear in

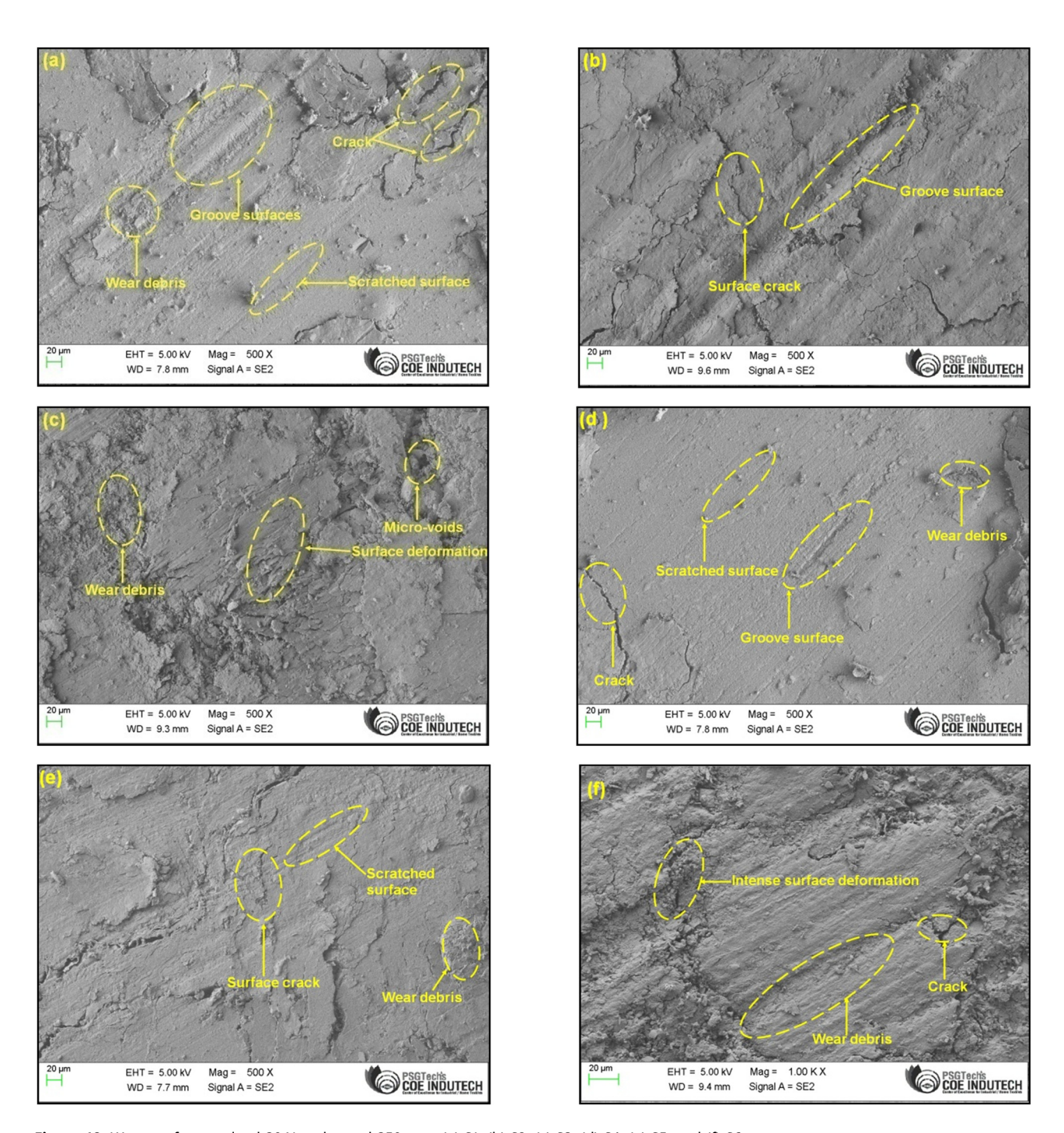


Figure 12: Worn surfaces at load 30 N and speed 350 rpm: (a) S1, (b) S2, (c) S3, (d) S4, (e) S5, and (f) S6.

the S3 at higher loading conditions. Singh *et al.* [38] observed that as the normal load and sliding speed increased, the formation of surface deformation increased during the dry wear of sisal fiber composites. Figure 12(d) demonstrates the worn surface of S4 composites. Less wear debris and a smaller portion of grooved surfaces were noticed in the SEM of S4. The combination of fly ash and WC filler improved the wear resistance of sisal fiber composites, particularly under

conditions of increased loading. From the worn surface, it was confirmed that during wear, both fillers prevented the matrix contact area from thermal and mechanical failures. Therefore, the wear rate of S4 composites was less than that of other composites. The surface cracks and wear debris are seen in the worn surface (Figure12(e)) of S5 composites. During high loading conditions, the influence of basalt powder in the S5 composite was high compared to fly ash.

Hence, it was confirmed by the formation of scaling layers and the absence of grooved surfaces. The worn surface pattern of the S6 is similar to that of the S3, as shown in Figure 12(f). The intense surface deformation was formed due to direct contact with the composite surface on the disc. A similar kind of worn surface was noticed in Chang and Friedrich's [43] titanium oxide filler-reinforced composites. The occurrence of wear debris in the S6 confirms that hybridization fillers such as WC and basalt powder had no effect compared to the other two composites (S4 and S5).

The automotive sector is one of the main industries where sisal fiber composites are used. These composite materials are used to make interior parts like door panels, dashboards, and seat backs [44-46]. The composites are ideal for these automotive applications because the addition of fly ash, basalt powder, and tungsten carbide enhances their mechanical strength, stiffness, and impact resistance [47-49]. Sisal is one of many natural fibers that are employed because they reduce the use of synthetic materials, which has a positive impact on the environment [50.51].

The construction sector is another application for sisal fiber composites. Building supplies like roofing sheets, wall panels, and floor tiles are made with the help of composites [52-54]. The strength, fire resistance, and thermal insulation of the composite materials are enhanced by blending fly ash, basalt powder, and tungsten carbide with sisal fibers [55-57]. They can thus withstand extreme environmental conditions and enhance buildings' energy efficiency [58,59].

The use of sisal fiber composites in the aerospace sector is advantageous. In the production of aircraft interiors, such as cabin panels, overhead bins, and seating components, these composite materials are used [60-62]. Fly ash, basalt powder, and tungsten carbide are combined to give the composites high strength-to-weight ratio properties, resulting in lightweight yet sturdy structures [63–65]. The use of sisal fibers also helps the aerospace industry become more sustainable and reduce its carbon footprint [66-68].

Additionally, sisal fiber composites with fly ash, basalt powder, and tungsten carbide additives are used in a variety of consumer goods and sporting goods [69-71]. Items like furniture, toys, sporting goods, and musical instruments are all made using the composites. The exceptional blend of materials enhances the products' strength, impact resistance, and aesthetic appeal [72–74].

All in all, the use of sisal fiber composites combined with fly ash, basalt powder, and tungsten carbide using the compression molding process method has a variety of applications in industries like automotive, construction, aerospace, as well as consumer goods and sporting goods [75–77]. These composites are an excellent alternative for many manufacturing applications because of their enhanced mechanical properties, environmental sustainability, and improved performance [78,79].

4 Conclusion

The sisal fiber composites were incorporated with fly ash. basalt powder, and WC using the compression molding process method, following mechanical results. Fly ash, basalt, and WC filler powders mixed with 30% sisal fiber exhibited exceptional mechanical and wear properties. The addition of base powder produced the highest tensile strength of 112.2 MPa, while the addition of WC powder produced the lowest tensile strength of 86.3 MPa. The hybrid filler-added composite had a lower tensile strength than the single filler-added composite. The agglomeration of fillers in the composite causes a reduction in the tensile strength.

- 1) Similarly, 7.26, 17.64, 9.71, 18.58, 19.94, and 14.186% enhancements in flexural strength were observed with fly ash, basal powder, WC, fly ash + WC, fly ash + basalt, and WC + basalt. The hybrid filler-substituted (fly ash + basalt) sisal fiber composite was shown to have improved flexural strength.
- 2) The maximum impact strength of 5.34 kJ·m⁻² was observed when fly ash and basalt filler powders were substituted. The lowest impact strength was observed in the fly ash filler added sisal fiber composite.
- 3) Shore D hardness was improved by 3.375% (fly ash), 11.149% (basalt), 2.15% (WC), 5.73% (fly ash + WC), 9.05% (fly ash + basalt), and 6.86% (WC + basalt) for composites with filler added.
- 4) The S4 (fly ash + WC) composite is less wear resistance than the S1 composite.
- The tensile samples' SEM fractography revealed the river pattern, fiber breakage, fiber tear, and pull out, confirming that the addition of filler enhanced bonding, and the tensile failure was dominated by ductile.
- The least wear rate of the S2 composite was higher than S5 and S6. The hybridization of filler material was the reason for a slight increase in wear resistance of S5 and S6.
- 7) Wear debris in the S6 confirms that hybridization fillers such as WC and basalt powder had no effect compared to the other two composites (S4 and S5).

Acknowledgments: The authors extend their appreciation to the Deanship of Scientific Research at King Khalid University (KKU) for funding this research through the Research Group Program Under the Grant Number: (R.G.P.2/513/44).

Funding information: This research was funded by the Deanship of Scientific Research at King Khalid University (KKU) through the Research Group Program Under the Grant Number: (R.G.P.2/513/44).

Author contributions: All authors have accepted responsibility for the entire content of this manuscript and approved its submission.

Conflict of interest: The authors state no conflict of interest.

References

- [1] Ganapathy, T., R. Sathiskumar, M. R. Sanjay, P. Senthamaraikannan, S. S. Saravanakumar, J. Parameswaranpillai, et al. Effect of graphene powder on banyan aerial root fibers reinforced epoxy composites. *Journal of Natural Fibers*, Vol. 18, No. 7, 2021 Jul 3, pp. 1029–1036.
- [2] Mugesh Raja, V. and S. Sathees Kumar. Exploration of mechanical attributes, thermal behaviors and atomic force analysis of alkali treated hybrid polyester composites for an engineering application. Fibers and Polymers, Vol. 22, No. 9, 2021 Sep. pp. 2535–2542.
- [3] Sathees Kumar, S. Effect of natural fiber loading on mechanical properties and thermal characteristics of hybrid polyester composites for industrial and construction fields. Fibers and Polymers, Vol. 21, 2020 Jul, pp. 1508–1514.
- [4] Magarajan, U., D. Arvind, N. Kannan, and P. Hemanandan. A comparative study on the static mechanical properties of glass fibre vs glass-jute fibre polymer composite. *Materials Today:* Proceedings, Vol. 5, No. 2, 2018 Jan 1, pp. 6711–6716.
- [5] Kumaresan, M., S. Sathish, and N. Karthi. Effect of fiber orientation on mechanical properties of sisal fiber reinforced epoxy composites. *Journal of Applied Science and Engineering*, Vol. 18, No. 3, 2015 Sep, pp. 289–294.
- [6] Jagadeesh, P., M. Puttegowda, P. Boonyasopon, S. M. Rangappa, A. Khan, and S. Siengchin. Recent developments and challenges in natural fiber composites: A review. *Polymer Composites*, Vol. 43, No. 5, 2022 May, pp. 2545–2561.
- [7] Sanjay, M. R., G. R. Arpitha, L. L. Naik, K. Gopalakrishna, and B. J. Yogesha. Applications of natural fibers and its composites: an overview. *Natural Resources*, Vol. 7, No. 3, 2016 Mar 11, pp. 108–114.
- [8] Sanjay, M. R., P. Madhu, M. Jawaid, P. Senthamaraikannan, S. Senthil, and S. Pradeep. Characterization and properties of natural fiber polymer composites: A comprehensive review. *Journal of Cleaner Production*, Vol. 172, 2018 Jan 20, pp. 566–581.
- [9] Ahmad, F., N. Yuvaraj, and P. K. Bajpai. Effect of reinforcement architecture on the macroscopic mechanical properties of fiberous polymer composites: A review. *Polymer Composites*, Vol. 41, No. 6, 2020 Jun, pp. 2518–2534.

- [10] Choudhary, M., T. Singh, A. Sharma, M. Dwivedi, and A. Patnaik. Evaluation of some mechanical characterization and optimization of waste marble dust filled glass fiber reinforced polymer composite. *Materials Research Express*, Vol. 6, No. 10, 2019 Aug 7, id. 105702.
- [11] Sharma, A. and A. Patnaik. Experimental investigation on mechanical and thermal properties of marble dust particulate-filled needle-punched nonwoven jute fiber/epoxy composite. *Jom*, Vol. 70, No. 7, 2018 Jul, pp. 1284–1288.
- [12] Aslan, M. U., M. Tufan, and T. Küçükömeroğlu. Tribological and mechanical performance of sisal-filled waste carbon and glass fibre hybrid composites. *Composites Part B: Engineering*, Vol. 140, 2018 May 1, pp. 241–249.
- [13] Sumesh, K. R., V. Kavimani, G. Rajeshkumar, P. Ravikumar, and S. Indran. An investigation into the mechanical and wear characteristics of hybrid composites: influence of different types and content of biodegradable reinforcements. *Journal of Natural Fibers*, Vol. 19, No. 8, 2022 Aug 3, pp. 2823–2835.
- [14] Sumesh, K. R., V. Kavimani, G. Rajeshkumar, S. Indran, and A. Khan. Mechanical, water absorption and wear characteristics of novel polymeric composites: impact of hybrid natural fibers and oil cake filler addition. *Journal of Industrial Textiles*, Vol. 51, No. 4_suppl, 2022 Jun, pp. 5910S–5937S.
- [15] Nguyen, H., M. Jamali Moghadam, and H. Moayedi. Agricultural wastes preparation, management, and applications in civil engineering: a review. *Journal of Material Cycles and Waste Management*, Vol. 21, 2019 Sep 13, pp. 1039–1051.
- [16] Mittal, V., R. Saini, and S. Sinha. Natural fiber-mediated epoxy composites—a review. *Composites Part B: Engineering*, Vol. 99, 2016 Aug 15, pp. 425–435.
- [17] Senthilkumar, K., N. Saba, N. Rajini, M. Chandrasekar, M. Jawaid, S. Siengchin, and O. Y. Alotman. Mechanical properties evaluation of sisal fibre reinforced polymer composites: A review. *Construction and Building Materials*, Vol. 174, 2018 Jun 20, pp. 713–729.
- [18] Bessell, T. J. and S. M. Mutuli. The interfacial bond strength of sisal —cement composites using a tensile test. *Journal of Materials Science Letters*, Vol. 1, No. 6, 1982 Jun, pp. 244–246.
- [19] Sumesh, K. R., V. Kavimani, G. Rajeshkumar, S. Indran, and G. Saikrishnan. Effect of banana, pineapple and coir fly ash filled with hybrid fiber epoxy based composites for mechanical and morphological study. *Journal of Material Cycles and Waste Management*, Vol. 23, 2021 Jul, pp. 1277–1288.
- [20] Staiger, M. P. and N. Tucker. Natural-fibre composites in structural applications. *In Properties and performance of natural-fibre compo*sites, Woodhead Publishing, Sawston, United Kingdom, 2008 Jan 1, pp. 269–300.
- [21] Mishra, S., A. K. Mohanty, L. T. Drzal, M. Misra, and G. Hinrichsen. A review on pineapple leaf fibers, sisal fibers and their biocomposites. *Macromolecular Materials and Engineering*, Vol. 289, No. 11, 2004 Nov 19, pp. 955–974.
- [22] Noorunnisa Khanam, P., H. P. Abdul Khalil, G. Ramachandra Reddy, and S. Venkata Naidu. Tensile, flexural and chemical resistance properties of sisal fibre reinforced polymer composites: effect of fibre surface treatment. *Journal of Polymers and the Environment*, Vol. 19, 2011 Mar, pp. 115–119.
- [23] Yusriah, L., S. M. Sapuan, E. S. Zainudin, and M. Mariatti. Characterization of physical, mechanical, thermal and morphological properties of agro-waste betel nut (Areca catechu) husk fibre. Journal of Cleaner Production, Vol. 72, 2014 Jun 1, pp. 174–180.
- [24] Chandrasekar, M., M. R. Ishak, S. M. Sapuan, Z. Leman, and M. lawaid. A review on the characterisation of natural fibres and their

- composites after alkali treatment and water absorption. Plastics, Rubber and Composites, Vol. 46, No. 3, 2017 Mar 16, pp. 119-136.
- [25] Maurya, A. K., R. Gogoi, and G. Manik. Mechano-chemically activated fly-ash and sisal fiber reinforced PP hybrid composite with enhanced mechanical properties. Cellulose, Vol. 28, 2021 Sep, pp. 8493-8508.
- [26] Devaraju, A. and P. Sivasamy. Comparative analysis of mechanical characteristics of sisal fibre composite with and without nano particles. Materials Today: Proceedings, Vol. 5, No. 6, 2018 Jan 1, pp. 14362-14366.
- [27] Ji, M., F. Li, J. Li, J. Li, C. Zhang, K. Sun, et al. Enhanced mechanical properties, water resistance, thermal stability, and biodegradation of the starch-sisal fibre composites with various fillers. Materials & Design, Vol. 198, 2021 Ian 15, id. 109373.
- [28] Alemayehu, Z., R. B. Nallamothu, M. Liben, S. K. Nallamothu, and A. K. Nallamothu. Experimental investigation on characteristics of sisal fiber as composite material for light vehicle body applications. Materials Today: Proceedings, Vol. 38, 2021 Jan 1, pp. 2439-2444.
- [29] Athith, D., M. R. Sanjay, T. G. Yashas Gowda, P. Madhu, G. R. Arpitha, B. Yogesha, et al. Effect of tungsten carbide on mechanical and tribological properties of jute/sisal/E-glass fabrics reinforced natural rubber/epoxy composites. Journal of Industrial Textiles, Vol. 48, No. 4, 2018 Oct, pp. 713-737.
- [30] Vivek, S. and K. Kanthavel. Effect of bagasse ash filled epoxy composites reinforced with hybrid plant fibres for mechanical and thermal properties. Composites Part B: Engineering, Vol. 160, 2019 Mar 1, pp. 170-176.
- [31] Haldar, P., N. Modak, and G. Sutradhar. Comparative evaluation of mechanical properties of sisal-epoxy composites with and without addition of aluminium powder. Materials Today: Proceedings, Vol. 4, No. 2, 2017 Jan 1, pp. 3397-3406.
- [32] Oladele, I. O., B. A. Makinde-Isola, A. A. Adediran, M. O. Oladejo, A. F. Owa, and T. M. Olayanju. Mechanical and wear behaviour of pulverised poultry eggshell/sisal fiber hybrid reinforced epoxy composites. Materials Research Express, Vol. 7, No. 4, 2020 Apr 14, id. 045304.
- [33] da Silva, L. J., T. H. Panzera, V. R. Velloso, A. L. Christoforo, and F. Scarpa. Hybrid polymeric composites reinforced with sisal fibres and silica microparticles. Composites Part B: Engineering, Vol. 43, No. 8, 2012 Dec 1, pp. 3436-3444.
- [34] Mohan, T. P. and K. Kanny. Water barrier properties of nanoclay filled sisal fibre reinforced epoxy composites. Composites Part A: Applied Science and Manufacturing, Vol. 42, No. 4, 2011 Apr 1, pp. 385-393.
- [35] Maharana, S. M., M. K. Pandit, and A. K. Pradhan. Influence of fumed silica nanofiller and stacking sequence on interlaminar fracture behaviour of bidirectional jute-kevlar hybrid nanocomposite. Polymer Testing, Vol. 93, 2021 Jan 1, id. 106898.
- [36] Rashid, B., Z. Leman, M. Jawaid, M. J. Ghazali, and M. R. Ishak. Physicochemical and thermal properties of lignocellulosic fiber from sugar palm fibers: Effect of treatment. Cellulose, Vol. 23, 2016 Oct, pp. 2905-2916.
- [37] Gupta, M. K. and R. K. Srivastava. Properties of sisal fibre reinforced epoxy composite. Indian Journal of Fibre & Textile Research, Vol. 41, No. 9, 2016.
- [38] Singh, T., B. Gangil, L. Ranakoti, and A. Joshi. Effect of silica nanoparticles on physical, mechanical, and wear properties of natural fiber reinforced polymer composites. Polymer Composites, Vol. 42, No. 5, 2021 May, pp. 2396-2407.
- [39] James, D. J. D., S. Manoharan, G. Saikrishnan, and S. Arjun. Influence of bagasse/sisal fibre stacking sequence on the

- mechanical characteristics of hybrid-epoxy composites. Journal of Natural Fibers, Vol. 17, No. 10, 2020 Oct 2, pp. 1497-1507.
- Megahed, A. A., M. A. Agwa, and M. Megahed. Improvement of [40] hardness and wear resistance of glass fiber-reinforced epoxy composites by the incorporation of silica/carbon hybrid nanofillers. Polymer-Plastics Technology and Engineering, Vol. 57, No. 4, 2018 Mar 4, pp. 251-259.
- [41] Govindan, P., A. Arul Jeya Kumar, and A. Lakshmankumar. Wear and morphological analysis on basalt/sisal hybrid fiber reinforced poly lactic acid composites. Proceedings of the Institution of Mechanical Engineers, Part L: Journal of Materials: Design and Applications, Vol. 236, No. 5, 2022 May, pp. 1053-1066.
- [42] Renukappa, N. M., B. Suresha, R. M. Devarajaiah, and K. N. Shivakumar. Dry sliding wear behaviour of organo-modified montmorillonite filled epoxy nanocomposites using Taguchi's techniques. Materials & Design, Vol. 32, No. 8-9, 2011 Sep 1, pp. 4528-4536.
- [43] Chang, L., K. Friedrich, and L. Ye. Study on the transfer film layer in sliding contact between polymer composites and steel disks using nanoindentation. Journal of Tribology, Vol. 136, No. 2, 2014 Apr 1, id. 021602.
- [44] Zhang, X., F. Ma, Z. Dai, J. Wang, L. Chen, H. Ling, et al. Radionuclide transport in multi-scale fractured rocks: A review. Journal of Hazardous Materials, Vol. 424, No. Pt C, 2022, id. 127550.
- Shi, J., B. Zhao, T. He, L. Tu, X. Lu, and H. Xu. Tribology and dynamic characteristics of textured journal-thrust coupled bearing considering thermal and pressure coupled effects. Tribology International, Vol. 180, 2023, id. 108292.
- [46] Peng, J., C. Xu, B. Dai, L. Sun, J. Feng, and Q. Huang. Numerical Investigation of Brittleness Effect on Strength and Microcracking Behavior of Crystalline Rock. International Journal of Geomechanics, Vol. 22, No. 10, 2022, id. 4022178.
- [47] Dai, Z., Z. Ma, X. Zhang, J. Chen, R. Ershadnia, X. Luan, et al. An integrated experimental design framework for optimizing solute transport monitoring locations in heterogeneous sedimentary media. Journal of Hydrology, Vol. 614, 2022, id. 128541.
- Zhang, X., Z. Wang, P. Reimus, F. Ma, M. R. Soltanian, B. Xing, et al. Plutonium reactive transport in fractured granite: Multi-species experiments and simulations. Water Research, Vol. 224, 2022, id. 119068.
- [49] Zhao, W., H. Suo, S. Wang, L. Ma, L. Wang, Q. Wang, et al. Mg gas infiltration for the fabrication of MgB2 pellets using nanosized and microsized B powders. Journal of the European Ceramic Society, Vol. 44, No. 10, 2018, pp. 11022-11029.
- [50] Zhang, P., Z. Liu, X. Yue, P. Wang, and Y. Zhai. Water jet impact damage mechanism and dynamic penetration energy absorption of 2A12 aluminum alloy. Vacuum, Vol. 206, 2022, id. 111532.
- [51] Yang, K., N. Qin, H. Yu, C. Zhou, H. Deng, W. Tian, et al. Correlating multi-scale structure characteristics to mechanical behavior of Caprinae horn sheaths. Journal of Materials Research and Technology, Vol. 21, 2022, pp. 2191-2202.
- [52] Jin, M., Y. Ma, W. Li, J. Huang, Y. Yan, H. Zeng, et al. Multi-scale investigation on composition-structure of C-(A)-S-H with different Al/Si ratios under attack of decalcification action. Cement and Concrete Research, Vol. 172, 2023, id. 107251.
- [53] Jia, S., Z. Dai, Z. Zhou, H. Ling, Z. Yang, L. Qi, et al. Upscaling dispersivity for conservative solute transport in naturally fractured media. Water Research, Vol. 235, 2023, id. 119844.
- [54] Bai, X., H. Shi, K. Zhang, X. Zhang, and Y. Wu. Effect of the fit clearance between ceramic outer ring and steel pedestal on the

- sound radiation of full ceramic ball bearing system. *Journal of Sound and Vibration*, Vol. 529, 2022, id. 116967.
- [55] Bai, B., F. Bai, Q. Nie, and X. Jia. A high-strength red mud-fly ash geopolymer and the implications of curing temperature. *Powder Technology*, Vol. 416, 2023, id. 118242.
- [56] Xia, Y., M. Shi, C. Zhang, C. Wang, X. Sang, R. Liu, et al. Analysis of flexural failure mechanism of ultraviolet cured-in-place-pipe materials for buried pipelines rehabilitation based on curing temperature monitoring. *Engineering Failure Analysis*, Vol. 142, 2022, id. 106763.
- [57] Zhang, Z., W. Li, and J. Yang. Analysis of stochastic process to model safety risk in construction industry. *Journal of Civil Engineering and Management*, Vol. 27, No. 2, 2021, pp. 87–99.
- [58] Lu, Z., D. Gu, H. Ding, W. Lacarbonara, and L. Chen. Nonlinear vibration isolation via a circular ring. Mechanical Systems and Signal Processing, Vol. 136, 2020, id. 106490.
- [59] Xu, P., Q. Yuan, W. Ji, R. Yu, F. Wang, and N. Huo. Study on the annealing phase transformation mechanism and electrochemical properties of carbon submicron fibers loaded with cobalt. *Materials Express*, Vol. 12, No. 12, 2022, pp. 4–13.
- [60] Zhao, Y., J. Jing, L. Chen, F. Xu, and H. Hou. Current research status of interface of ceramic-metal laminated composite material for armor protection. *Jinshu Xuebao/Acta Metallurgica Sinica*, Vol. 57, 2021, pp. 1107–1125.
- [61] Li, M., Q. Guo, L. Chen, L. Li, H. Hou, and Y. Zhao. Microstructure and properties of graphene nanoplatelets reinforced AZ91D matrix composites prepared by electromagnetic stirring casting. *Journal of Materials Research and Technology*, Vol. 21, 2022, pp. 4138–4150.
- [62] Chen, L., Y. Zhao, J. Jing, and H. Hou. Microstructural evolution in graphene nanoplatelets reinforced magnesium matrix composites fabricated through thixomolding process. *Journal of Alloys and Compounds*, Vol. 940, 2023, id. 168824.
- [63] Zhang, C., H. Khorshidi, E. Najafi, and M. Ghasemi. Fresh, mechanical and microstructural properties of alkali-activated composites incorporating nanomaterials: A comprehensive review. *Journal of Cleaner Production*, Vol. 384, 2023, id. 135390.
- [64] Zhang, H., Y. Xiao, Z. Xu, M. Yang, L. Zhang, L. Yin, et al. Effects of Nidecorated reduced graphene oxide nanosheets on the microstructural evolution and mechanical properties of Sn-3.0Ag-0.5Cu composite solders. *Intermetallics*, Vol. 150, 2022, id. 107683.
- [65] Deng, H., Y. Chen, Y. Jia, Y. Pang, T. Zhang, S. Wang, et al. Microstructure and mechanical properties of dissimilar NiTi/ Ti6Al4V joints via back-heating assisted friction stir welding. *Journal of Manufacturing Processes*, Vol. 64, 2021, pp. 379–391.
- [66] Long, X., Y. Guo, Y. Su, K. S. Siow, and C. Chen. Unveiling the damage evolution of SAC305 during fatigue by entropy generation. *International Journal of Mechanical Sciences*, Vol. 244, 2023, id. 108087.

- [67] Yao, Z. and H. Yoon. Hybrid Electric Vehicle Powertrain Control Based on Reinforcement Learning. SAE International Journal of Electrified Vehicles, Vol. 11, No. 2, 2021, pp. 165–176.
- [68] Li, X., C. Du, X. Wang, and J. Zhang. Quantitative determination of high-order crack fabric in rock plane. *Rock Mechanics and Rock Engineering*, 2023, pp. 1–10.
- [69] Fu, Z. H., B. J. Yang, M. L. Shan, T. Li, Z. Y. Zhu, C. P. Ma, et al. Hydrogen embrittlement behavior of SUS301L-MT stainless steel laser-arc hybrid welded joint localized zones. *Corrosion Science*, Vol. 164, 2020, id. 108337.
- [70] Zhang, X., Y. Xiong, Y. Pan, H. Du, and B. Liu. Crushing stress and vibration fatigue-life optimization of a battery-pack system. Structural and Multidisciplinary Optimization, Vol. 66, 2023, pp. 48.
- [71] Liao, D., S. Zhu, B. Keshtegar, G. Qian, and Q. Wang. Probabilistic framework for fatigue life assessment of notched components under size effects. *International Journal of Mechanical Sciences*, Vol. 181, 2020, id. 105685.
- [72] Niu, X., S. Zhu, J. He, D. Liao, J. A. F. O. Correia, F. Berto, et al. Defect tolerant fatigue assessment of AM materials: Size effect and probabilistic prospects. *International Journal of Fatigue*, Vol. 160, 2022. id. 106884.
- [73] He, J., S. Zhu, C. Luo, X. Niu, and Q. Wang. Size effect in fatigue modelling of defective materials: Application of the calibrated weakest-link theory. *International Journal of Fatigue*, Vol. 165, 2022, id. 107213.
- [74] Jiang, H., M. Wang, P. Zhao, Z. Xiao, and S. Dustdar. A utility-aware general framework with quantifiable privacy preservation for destination prediction in LBSs. *IEEE/ACM Trans Netw*, Vol. 29, No. 5, 2021, pp. 2228–2241.
- [75] Shao, Z., J. Chen, Q. Xie, and L. Mi. Functional metal/covalent organic framework materials for triboelectric nanogenerator. *Coordination Chemistry Reviews*, Vol. 486, 2023, id. 215118.
- [76] Li, Z., Y. Kong, and C. Jiang. A transfer double deep Q network based DDoS detection method for internet of vehicles. *IEEE Transactions on Vehicular Technology*, Vol. 72, No. 4, 2023, pp. 5317–5331.
- [77] Jiang, S., C. Zhao, Y. Zhu, C. Wang, Y. Du, W. Lei, et al. A practical and economical ultra-wideband base station placement approach for indoor autonomous driving systems. *Journal of advanced transportation*, Vol. 2022, 2022, pp. 1–12.
- [78] Hu, Z., G. He, X. Zhang, T. Huang, H. Li, Y. Zhang, et al. Impact behavior of nylon kernmantle ropes for high-altitude fall protection. *Journal of Engineered Fibers and Fabrics*, Vol. 18, 2023, id. 15589250231167401.
- [79] Hou, X., L. Zhang, Y. Su, G. Gao, Y. Liu, Z. Na, et al. A space crawling robotic bio-paw (SCRBP) enabled by triboelectric sensors for surface identification. *Nano Energy*, Vol. 105, 2023, id. 108013.